Journal of the Neurological Sciences 405 (2019) 116433

Contents lists available at ScienceDirect

Journal of the Neurological Sciences

journal homepage: www.elsevier.com/locate/jns

Cerebral blood volume and apparent diffusion coefficient – Valuable predictors of non-response to bevacizumab treatment in patients with recurrent glioblastoma

Lucie Petrova[a,g], Panagiotis Korfiatis[b], Ondra Petr[c], Daniel H. LaChance[d], Ian Parney[e], Jan C. Buckner[f], Bradley J. Erickson[b,*]

[a] Department of Anesthesiology and Critical Care Medicine, Medical University Innsbruck, 6020 Innsbruck, Austria
[b] Department of Radiology, Mayo Clinic, 200 First St SW, Rochester, MN 55905, United States of America
[c] Department of Neurosurgery, Medical University Innsbruck, 6020 Innsbruck, Austria
[d] Department of Neurology, Mayo Clinic, 200 First St SW, Rochester, MN 55905, United States of America
[e] Department of Neurosurgery, Mayo Clinic, 200 First St SW, Rochester, MN 55905, United States of America
[f] Department of Oncology, Mayo Clinic, 200 First St SW, Rochester, MN 55905, United States of America
[g] Austria and Department of Neurosurgery, Military Hospital in Prague, 16902 Praha 6, Czech Republic

ARTICLE INFO

Keywords:
Glioblastoma multiforme
Bevacizumab
Cerebral blood volume
Apparent diffusion coefficient
Glioma therapy response
Machine learning

ABSTRACT

Background: Glioblastoma multiforme (GBM) is the most common primary brain tumor in adults. The core of standard of care for newly diagnosed GBM was established in 2005 and includes maximum feasible surgical resection followed by radiation and temozolomide, with subsequent temozolomide with or without tumor-treating fields. Unfortunately, nearly all patients experience a recurrence. Bevacizumab (BV) is a commonly used second-line agent for such recurrences, but it has not been shown to impact overall survival, and short-term response is variable.

Methods: We collected MRI perfusion and diffusion images from 54 subjects with recurrent GBM treated only with radiation and temozolomide. They were subsequently treated with BV. Using machine learning, we created a model to predict short term response (6 months) and overall survival. We set time thresholds to maximize the separation of responders/survivors versus non-responders/short survivors.

Results: We were able to segregate 21 (68%) of 31 subjects into unlikely to respond categories based on Progression Free Survival at 6 months (PFS6) criteria. Twenty-two (69%) of 32 subjects could similarly be identified as unlikely to survive long using the machine learning algorithm.

Conclusion: With the use of machine learning techniques to evaluate imaging features derived from pre- and post-treatment multimodal MRI, it is possible to identify an important fraction of patients who are either highly unlikely to respond, or highly likely to respond. This can be helpful is selecting patients that either should or should not be treated with BV.

1. Introduction

Glioblastoma multiforme (GBM) remains the most common primary brain tumor. The core of standard of care for newly diagnosed glioblastoma was established in 2005 [1,2] and includes maximal safe surgical resection followed by radiation and temozolomide, with subsequent temozolomide chemotherapy with or without tumor-treating fields [3]. However, nearly all patients experience recurrence and criteria for selecting second-line therapy are less clear [4]. Management options for recurrent disease that have been limited, have been recently enhanced through the advent of targeted therapies [5,6].

One of these treatment option at recurrence in some countries is bevacizumab (BV), an inhibitor of vascular endothelial growth factor developed to block angiogenesis [7]. The noncomparative randomized phase II, multicenter, open-label BRAIN trial (AVF3708g) investigating bevacizumab plus irinotecan versus bevacizumab alone [8,9] contributed to accelerated FDA approval of bevacizumab (Avastin®, Genentech) for treatment of recurrent glioblastoma in 2009. Despite its current US approval for treatment of recurrent glioblastoma, phase II and III clinical trials for patients with recurrent glioblastoma [10], as

* Corresponding author.
E-mail address: bje@mayo.edu (B.J. Erickson).

https://doi.org/10.1016/j.jns.2019.116433
Received 22 April 2019; Received in revised form 30 July 2019; Accepted 22 August 2019
Available online 23 August 2019

well as 2 recent phase III randomized clinical trials for patients with newly diagnosed glioblastoma [5,6] showed no advance in overall survival (OS) with the addition of bevacizumab to standard therapy. While some patients do appear to have symptomatic improvement from bevacizumab (BV) therapy, its value for treating the tumor is less clear. It can be assumed that there is a patient population with a meaningful clinical benefit, given that the demonstrated activity of bevacizumab evidenced by impact on imaging-based endpoints [11-13]. Thus, identifying those subjects who are likely to respond or not respond is essential for the best management of glioblastoma patients.

Conventional MR imaging (T1, T2, contrast enhancement) as a standard imaging method for assessing response for glioblastomas has shown to be not always able to accurately assess tumor response. In particular, anti-angiogenic agents often cause improvement in blood-brain barrier (BBB) disruption and thus reduces contrast enhancement and edema, even when the tumor burden and viability is not impacted [5,6,10]. Development of imaging biomarkers that could anticipate response to therapy, have substantial prognostic value, or can recognize patients unlikely to respond to any therapy would be an extremely valuable tool in this regard.

In this paper, we used the novel imaging methods, along with machine learning, to assess the usefulness of the combination of Apparent Diffusion Coefficient (ADC) and dynamic-susceptibility contrast (DSC) perfusion MRI-based measurements to predict which patients with recurrent glioblastoma might respond to BV with respect to both progression free and overall survival.

2. Methods

2.1. Patient selection

After obtaining Institutional Review Board approval, we conducted a retrospective analysis of patients with recurrent glioblastoma treated at our institution from 2008 to 2016. A total of 54 consecutive patients who met the following criteria were identified and included in the study: (a) age of at least 18 years, (b) histologically confirmed contrast-enhancing glioblastoma based on the WHO histological grading system, (c) first recurrence of the tumor defined based on the updated RANO-criteria [14,15], never exposed to any other antiangiogenic therapy, after initial treatment according to current standard of care therapy (maximal safe surgical resection > 90% of tumor confirmed by post-operative MRI within 48 h after surgery, radiation therapy, and concomitant and adjuvant chemotherapy with temozolomide, (d) bevacizumab (Avastin®, Roche; 10 mg/kg body weight every 2 weeks intravenously) as second-line mono-therapy of the recurrent glioblastoma, (e) MRI examination including diffusion and DSC perfusion images < 3 weeks prior to switch to BV therapy, and at least 8 weeks between completion of radiotherapy and initiation of BV-therapy, (f) if receiving corticosteroids, stable or decreasing steroid dose for at least 5 days prior to the baseline MRI scan, (g) baseline Karnofsky performance status ≥ 70, (h); follow-up of at least one year or to time of death as well as clinical status during follow-up to allow assessment of PFS6. Of note, BV had to be administered because of tumor progression on temozolomide, not for the purpose of reducing edema such as in steroid-resistant edema.

Patients were excluded from this study if (a) a repeat surgery was performed before initiation of treatment or between the baseline and first follow-up imaging evaluation, (b) there was a recurrence 3 months or less from the end of radiation therapy to avoid involving cases with pseudoprogression, (c) MR images were of insufficient quality due to motion artifacts and/or due to missing advanced MR-sequences, (c) other or combined anti-angiogenic agents were applied.

2.2. Response criteria

We identified 54 subjects that met all above-mentioned criteria. Twenty-three (23) of these 54 patients did not progress within 6 months of initiating BV therapy based on clinical as well as radiologic assessment (including in-depth image review by senior consultant) and were referred to as 'responders'/'Long PFS6. Of note, twenty-two of the 54 subjects survived more than 12 months after initiating therapy, and these were referred to as 'OS Long'. The time periods for separating long and short are commonly used for both PFS6 and OS, and also divided our subjects into approximately equal groups.

2.3. Image processing

All images were retrieved from our clinical image archive, local identifiers were replaced with study identifiers, and stored in our research management system [16]. The T1 post-contrast images were processed with N4 bias correction [17] and intensity normalized. The contrast-enhancing region of interest (CEROI) was manually delineated by an expert without knowledge of the patient response status utilizing ITK snap [18]. The CEROI included the enhancing part of the tumor but did not include scar tissue or vessels.

The MR images on all patients were acquired with either 1.5 T or 3 T scanners for clinical care purposes. The diffusion-weighted images were all acquired with B = 1000, a 128 × 128 matrix that covered the whole brain (typically 22-24 cm) with a slice thickness of 5 mm. Apparent Diffusion Coefficient (ADC) maps were calculated from diffusion weighted trace images. These were then registered to the T1 weighted post-contrast images using ANTs [19]. We calculated the mean, median, 95th and 20th percentile values for ADC pixels corresponding to the CEROI, referred to as ADCmn, ADCmed, ADC95, ADC20 [20].

We computed relative cerebral blood volume (rCBV), K2, and Peak Signal Recovery (PSR) images from the dynamic susceptibility contrast (DSC) source images [20]. The dynamic susceptibility contrast (DSC) images were acquired with a 128 × 128 matrix to cover the brain, and with 10–12 slices that were 5 mm thick with 1 mm gap, to cover the tumor. The DSC images were obtained using a spin-echo echo-planar sequence with axial orientation and TR/TE/FA of 2217 to 2225 ms/60 ms/90 deg. A gadolinium bolus of 0.1 mmol was injected followed by 20 cc saline, with the bolus beginning 10 s after the beginning of the acquisition (which allows establishment of baseline intensity).

The DSC acquisitions and corresponding maps were registered to the T1-post contrast images also using ANTs [19]. A reference white matter area was created at a location corresponding to the CEROI but in the opposite hemisphere white matter when possible; else the opposite hemisphere on the same slice where white matter appeared normal. Each pixel in the CBV image was divided by the mean value of the white matter region to produce the rCBV image. We calculated the mean, median and the 95th percentile intensity on the rCBV image for the CEROI.

The K2 image, computed as the slope of the baseline after the bolus peak, reflects the slow leakage of contrast material into tissue and is somewhat analogous to K_{trans}. Finally, the Peak Signal Recovery, representing the fraction of baseline intensity versus the maximum signal loss for the enhancing tissue, was also calculated. An example of the T1 image and the corresponding ADC and rCBV images with CEROI is shown in Fig. 1.

2.4. Machine learning

We then trained 6 different classifiers for predicting both OS (short vs long) and for PFS6 (short vs long): Gradient Boosted (GB) [21], support vector machine (SVM) [22], decision tree classifier (DT) [23], k-nearest neighbor (kNN) [24], passive aggressive classifier (PAC) [25], and logistic regression (LR) [26]. These classifiers were selected because they represent a wide variety of classifier styles and so if they had similar performance, it helps to assure that results are robust.

A 3 fold stratified cross validation [27] was used in order to train and select the best classifier from the six considered in the study. The

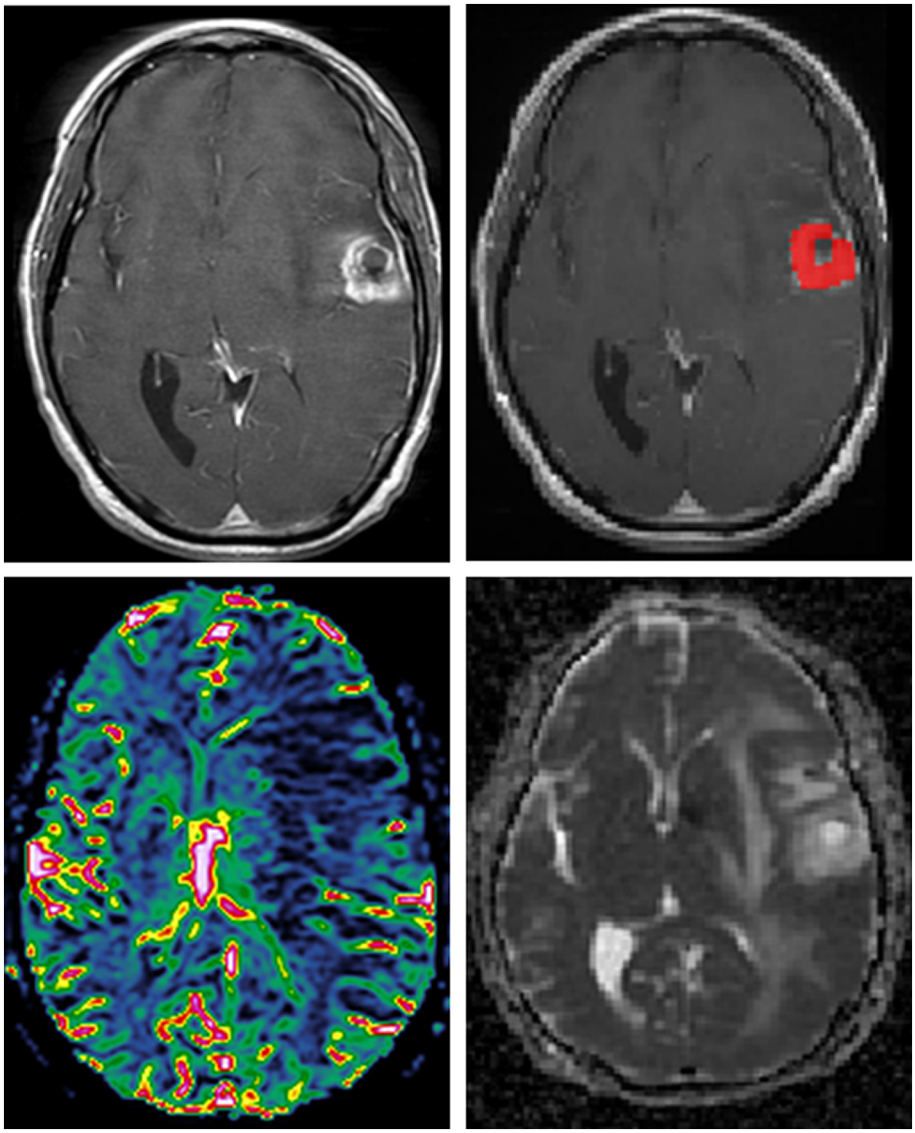

Fig. 1. The upper left image is the T1-weighted post-contrast image after undergoing bias correction and intensity normalization. The upper right figure shows the CEROI for this tumor superimposed on the post-contrast image. The lower left is the rCBV map for this subject and the lower right is the ADC map. This is a case where there was low rCBV and high ADC in a subject with ADC $>$ 2921, and was one of the 5 long survivors.

best classifier was that with the highest mean area under the receiver operating characteristic (ROC) curve for the 3 folds. The parameters of each classifier were also estimated utilizing grid search. The parameters include the k value for the KNN classifier, the σ and C for the SVM classifier as well as the number of estimators and the criterio used in the DT.

The sensitivity, specificity and overall accuracy were calculated. The ROC Curve that represents the overall performance of the system using the selected criteria was created to identify the point on that curve that had 100% sensitivity and a point where there was 100% specificity. These 2 points represent thresholds for classifying those highly likely to respond and also those highly likely to not respond.

3. Results

Among all included 54 subjects, 23 were 'responders' meaning that they did not meet criteria for progression at 6 months, and 22 were 'long survivors' meaning that they lived $>$ 1 year after being started on BV. We found that diffusion and perfusion imaging using an SVM was able to identify the imaging properties of subjects either highly likely to not progress within 6 months (PFS6) and those highly likely to progress These results are listed in Table 1. If the threshold of the SVM was set at 0.44, 13 (56.5%) of all 23 subjects that responded to BV-therapy could be identified, and at the same threshold, none (0%) of all 31 non-responders would be included (sensitivity 100%, specificity 0%). Conversely, if the threshold is set at 0.75, we would identify 21 (67.7%) of all 31 non-responders with none from the responders (sensitivity 0%, specificity 100%). Thus, by setting upper and lower thresholds, we were capable of identifying those subjects highly likely to not progress and those highly likely to progress. There were 20 (37.0%) subjects that had SVM values between 0.44 and 0.72 and of those, 10 (43.5%) were responders, and 10 (32.3%) were non-responders (sensitivity 50%, specificity 50%). The performance as measured by the area under the receiver operator characteristic curve for the 6 classifiers ranged from 0.84 to 0.91 for PFS6 and 0.76 to 0.83 for OS. While the SVM performed best for both OS and PFS6, the difference was not significant. We also note here that the variance of the performance across folds was not completely congruent suggesting the performance metrics are/are not reliable.

Performance of the classifier for predicting OS among all 22 'long

Table 1
Performance of SVM with separate thresholds for selecting subjects very likely/unlikely to respond (PFS6 Long) or to survive long (OS). In this group of 54 subjects, thresholds can identify 13/23 (57%) of subjects highly likely to respond, and 21/31 (68%) of those highly unlikely to respond. Among those that are neither highly likely to respond or not respond, there was a 50% chance of responding. For predicting OS, a threshold of 0.47 predicted 6 who were highly likely to survive long, and a threshold of 0.64 predicted 22 who were highly likely to not survive long. Among the remaining 26 subjects, 62% were long survivors.

	PFS6			
SVM Output	Responders	Non-responders	Sens	Spec
< 0.44	13	0	100%	0%
0.44–0.75	10	10	50%	50%
> 0.75	0	21	0%	100%
Total	23	31		
	OS			
SVM Output	Long Survivors	Short Survivors	Sens	Spec
< 0.47	6	0	100%	0%
0.47–0.64	16	10	62%	38%
> 0.64	0	22	0%	100%
Total	22	32		

survivors' was poorer, in that far more subjects were in the uncertain category. Using a threshold of 0.47, the system identified 6 (27.3%) long survivors with 0 (0%) short survivors (sensitivity 100%, specificity 0%), and a threshold of 0.64 identified 22 (68.8%) short survivors with 0 (0%) long survivors (sensitivity 0%, specificity 100%). Of 26 (48.1%) remaining subjects, 16 (72.7%) were long survivors and 10 (31.3%) were short survivors (sensitivity 62%, specificity 38%).

We found that diffusion and perfusion imaging using an SVM was able to identify 97% of subjects that would respond with an overall accuracy for PFS and OS of 0.82 and 0.78, respectively. The accuracy of the used 6 different classifiers ranged from 0.58 to 0.75 (OS) and 0.69 to 0.81 (PFS).

Table 2 shows the results when the SVM threshold was optimized for the binary (2 category) prediction of progression/no progression at 6 months (PFS6) or long/short survival (OS). This demonstrates certain ability to predict but may be less useful in clinical practice when compared to the aforementioned 3 categories that we described above. It also shows less power to predict OS than PFS6. The accuracy of the 6 different classifiers performing binary classification (will respond / won't respond) ranged from 0.58 to 0.75 (OS) and 0.69 to 0.81 (PFS6), respectively. The larger range for OS suggests that the imaging metrics were to a certain extent noisy for predicting OS, which might be not surprising given the numerous other factors that can affect survival.

Fig. 2 shows the various image metrics, and their performance in predicting OS and PFS6 in the particular case of GB classifier. The other classifiers tended to use the same features, though not all had the same top 3 features. There was almost no overlap of the top 3 features for predicting PFS6 versus those that best predicted OS. Of note, only ADC95 overlapped which was the most important predictor for OS, and 3rd most important for PFS6. However, while the exact metric was somewhat variable in all cases, ADC-based measures were always more informative than perfusion-based measures.

Fig. 3 shows the decision tree using simple thresholds on the computed diffusion or perfusion values for both OS and PFS6. While the performance of decision tree is not as high as SVM, it provides a human-interpretable basis for understanding imaging features used to make decisions. Fig. 3a, for instance, shows that for 5 subjects with ADCmn $> 2922 \times 10^{-6}$ mm [2]/s all 5 were long survivors. Of 49 subjects having ADCmn $< 2922 \times 10^{-6}$ mm^2/s, 7 subjects had ADCmed $< 1467 \times 10^{-6}$ mm^2/s and all 7 of those were short survivors.

Table 2
The performance of the optimized Support Vector optimized for high specificity. This allows high prediction of those who will not respond to BV. While the accuracy is only moderate, particularly for OS, this may be of value in identifying patients not likely to respond to BV.

Best SVM	OS	PFS6
Sens	0.62	0.61
Spec	0.88	0.97
Accuracy	0.78	0.82

4. Discussion

Recent evidence strongly suggests certain subpopulation of patients harboring recurrent glioblastoma with specific imaging characteristics that may have significant OS benefit from anti-VEGF therapy. Targeted anti-angiogenic therapies are, however, not without substantial cost and even serious toxicities. Bevacizumab is very expensive and treatment cost per patient may be up to 100,000.00US dollars per year [28]. We present a retrospective analysis of novel imaging methods, along with machine learning, to develop noninvasive quantitative prognostic biomarkers for survival and progression on the basis of the combination of Apparent Diffusion Coefficient (ADC) and dynamic-susceptibility contrast (DSC) perfusion MRI-based measurements. Results from the current study confirm that pre-treatment perfusion and diffusion MR-images are predictive imaging biomarkers for both progression-free survival and overall survival benefits in recurrent glioblastoma patients treated with bevacizumab. To our best knowledge, this is the first study using perfusion and diffusion images as well as 6 different classifier techniques to predict likelihood of response of recurrent glioblastoma, particularly with prior treatment using the standard radiation therapy and chemotherapy regimen.

We found that diffusion and perfusion imaging using an SVM was able to identify 97% of subjects that would respond with an overall accuracy for PFS and OS of 0.82 and 0.78, respectively. The accuracy of the used 6 different classifiers ranged from 0.58 to 0.75 (OS) and 0.69 to 0.81 (PFS). Not surprisingly, the imaging metrics were to a certain extent noisy for predicting OS given the numerous other factors that can affect survival rates. If 54 patients in our study are representative of all recurrent glioblastoma subjects, one could select more than two thirds of patients that are highly unlikely to respond to bevacizumab monotherapy. These subjects can benefit from renunciation of bevacizumab therapy that may be associated with rare but potentially serious toxicities [29,30].

Our study strictly focuses on metrics at the time of recurrence when BV therapy was contemplated. Being able to predict the success of BV therapy at the time of recurrence can avoid costs and complications of BV therapy and reduce delay to institute other therapies. Therefore, such a predictor would be of great value. It might also encourage those subjects who have the appropriate imaging findings to pursue anti-angiogenic therapy. Importantly, we found that using a combination of diffusion and perfusion, we could predict with high accuracy those subjects that would not likely benefit from BV, and those that likely would benefit from BV. Identifying these 2 subgroups from the full population of recurrent glioblastoma subjects can allowed more precise selection of best therapeutic options.

Of note, we studied 6 different classifier techniques, while most papers have used only 1 machine learning method for the classification task. We feel it is valuable to use several classifiers to help confirm robustness of findings. Given that there was no outlier in terms of performance (e.g. all the classifiers performed rather similarly), we believe the results are likely to be robust. If one or two classifiers were much better or worse than the others, that would suggest the results might be spurious and could cast doubts on the conclusions.

Fig. 3 shows the rather different decision criteria for PFS6 versus OS and that all classifiers performed worse when predicting OS than PFS6. But given that BV is known to improve PFS6 but not OS, maybe this

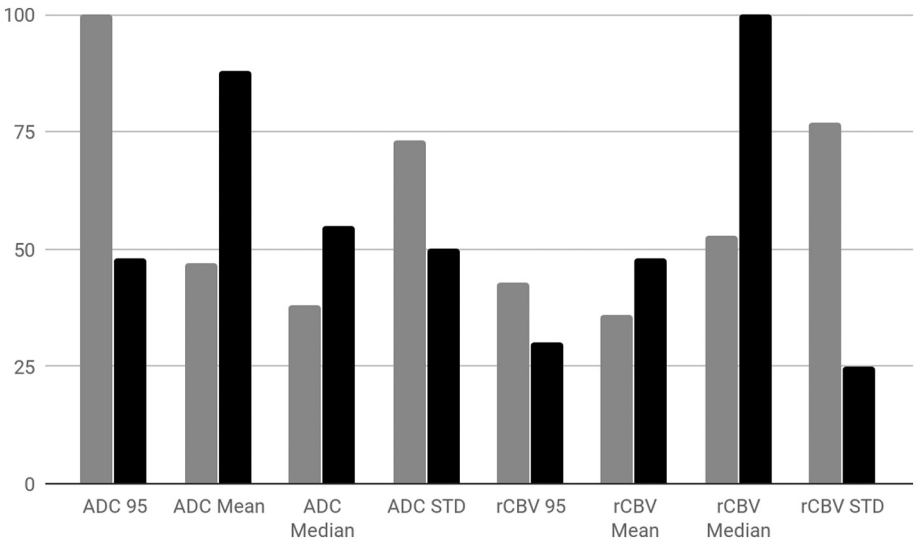

Fig. 2. Importance of various variables to prediction of OS (gray) and PFS (black). All values are scaled relative to the most important variable and are for the gradient boosted model. Other models had some differences in the top 3 predictors, suggesting that the predictors are noisy.

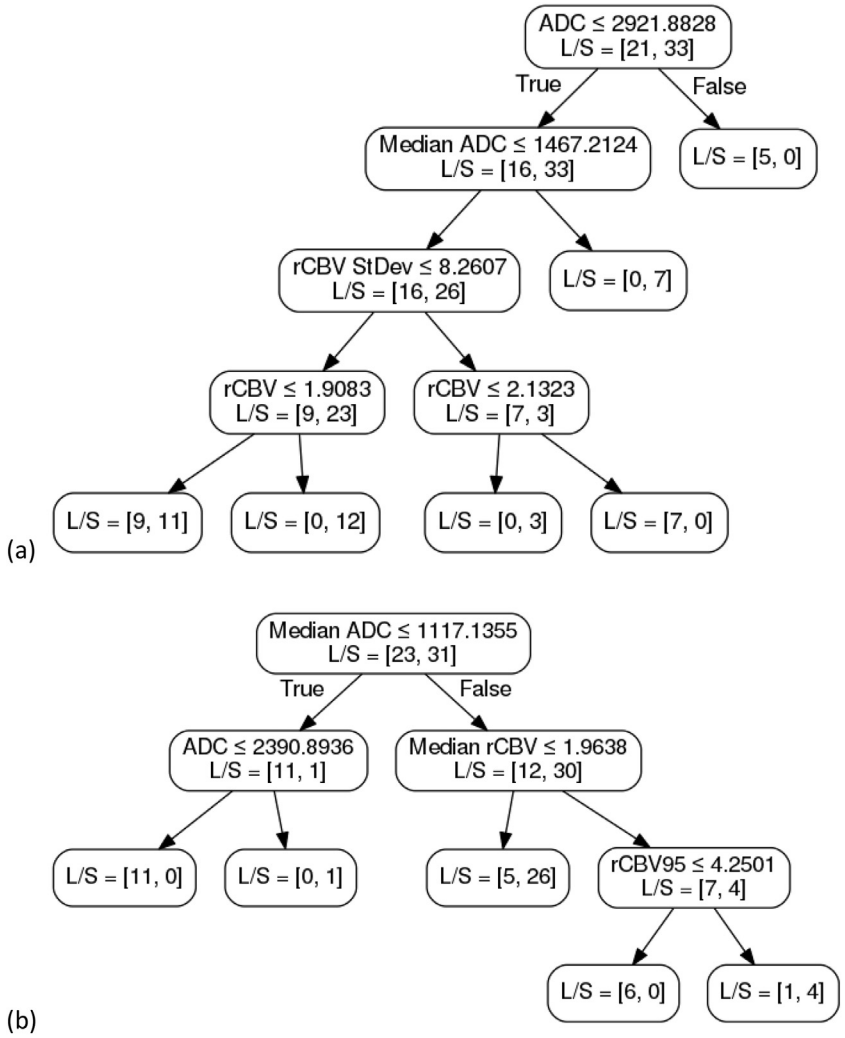

Fig. 3. Best decision tree based on random forest classifier for (a) OS and (b) PFS. For this figure, the first line in each block is the metric test, and the L/S refers to the number of subjects in the long survivors versus short survivors group. Note that this does not perform quite as well as the optimized SVM noted in Table 1, but is useful for understanding which image metrics are valuable and threshold values that may be used for simple yes/no decisions, compared to an SVM that performs more complex calculations to make its decision.

should not be so surprising. For OS, the total amount of tumor is probably most predictive, and might be reflected in the first decision point - whether there is much tissue without restricted diffusion (e.g. necrosis), they will live long (perhaps with or without BV). But for PFS6, the first decision focuses on how much tumor there is, and amount of restricted diffusion may be a good marker of that. If there is much restricted diffusion, one will likely get a radiographic response, even if there is not an OS benefit.

To our best knowledge, there have not been any published studies using perfusion and diffusion images to predict likelihood of response of recurrent glioblastoma, particularly with prior treatment using the current standard of care (STUPP-regimen). It is worthy of notice that numerous noninvasive imaging techniques have been used to stratify the markers of response and survival using anti-angiogenic treatment in patients with recurrent glioblastoma.

For example, Grossmann et al. [31] applied radiomics to clinical and imaging data from the multicenter BRAIN trial. This showed prognostic value for survival and progression in these patients receiving bevacizumab treatment. Goyal et al. [32] reported that the presence of homogenous dark signal (FDRn) on ADC maps at 8 weeks follow-up MRI correlated with a longer survival. The authors postulated that use of this qualitative diffusion signature in adjunct to contrast enhanced MRI may have the widest potential impact on routine clinical care for patients with recurrent high-grade gliomas. Galla et al. [33] showed that change in minimum ADC in the enhancing portion of the tumor after superselective intra-arterial bevacizumab therapy was associated with an increased risk of death (hazard ratio = 2.0, 95% confidence interval(CI) [1.04–3.79], $p = .038$), adjusting for age, tumor size, BV dose, and prior IV BV treatments. Field et al. [34] concluded that early progression on MRI appears to be a robust marker of a poor prognosis for patients on bevacizumab. Mardor et al. [35] described the use of diffusion weighted imaging (ADC and Radial diffusivity) from pre-treatment MRI, and showed mild correlation with response, defined as relative change in the tumor size, but they did not report PFS6 or OS. Additionally, only few authors [36–43] reported the prognostic value of PFS in patients with recurrent glioblastoma. In a pilot study of 16 patients with recurrent glioblastoma and antiangiogenic therapy with bevacizumab, Sawlani et al. [36] showed significantly improved correlation to TTP by using MR perfusion as compared with more commonly used metrics. Similarly, Bennet et al. [41] recently reported that changes in rCBV measures, especially load, correlated significantly with PFS and OS at follow-up time-points. Patients with the greatest reduction in $rCBV_{load}$ by 8-weeks of therapy had a significantly increased median OS (30 weeks; $p = .013$). The authors concluded that PWI may be of significant clinical utility in managing patients with recurrent glioblastoma, particularly those treated with anti-angiogenic agents such as bevacizumab. Finally, in the line with our study, using the machine learning techniques to analyze imaging features derived from pre- and posttherapy multimodal MRI, Chang et al. [11] developed a predictive model for patient OS that could potentially assist clinical decision making in patients with recurrent glioblastoma and anti-angiogenic bevacizumab therapy.

Despite improvements in PFS6, patients with glioblastoma treated with anti-angiogenic therapy eventually develop tumor progression. Two main types of resistance to anti-angiogenic therapy have been proposed: adaptive (evasive), in which the tumor acquires the ability to functionally evade the effects of angiogenic blockade, and inherent (intrinsic), which describes primary resistance to antiangiogenic therapy [44]. Potential mechanisms of resistance include upregulation of alternative proangiogenic pathways, leading to revascularization; recruitment of bone marrow-derived proangiogenic cells, thereby precluding the need for VEGF signaling; increased fibrosis and pericyte coverage to provide stabilization to the vessels; and change to an invasive phenotype to co-opt host vasculature [44,45].

Historically, the preferred method for assessing radiographic response in high-grade gliomas was based on the Macdonald criteria, which provided a standard measure of tumor response based on the product of the maximal cross-sectional diameters of the contrast-enhanced tumor margins from a disrupted BBB [46]. However, Macdonald criteria has several limitations in the presence of newer therapies [47,48]. To address some of these limitations, a Response Assessment in Neuro-Oncology Working Group proposed revised response criteria that are more useful for the assessment of antiangiogenic agents [14]. This represents one potential weakness in our results: while survival is quite clear, determining progression at 6 months (PFS6) can be challenging, particularly with anti-angiogenic therapy. In fact, a number of cases with short OS showed no radiographic progression, even on scans performed just a few weeks before death. For that reason, lack of seeing progression at 6 months is not a reliable outcome. However, the determination that there *is* progression is much more likely correct, and thus we feel comfortable that our tool's prediction of those likely to progress is reliable.

The advent of anti-angiogenic drugs held great promise as a way to 'starve' tumors by reducing blood flow and neovascularity. However, their value has not been clearly proven for all recurrent glioblastoma patients. In fact, one study of glioblastoma treated with anti-angiogenic agents showed that increased perfusion after initiation of therapy was correlated with longer PFS6 and OS [49] and another report showed that patients new glioblastoma treated with cediranib and chemoradiotherapy did better when they had increased perfusion [50]. Furthermore, in a phase II study of cediranib in patients with recurrent glioblastoma, a decrease in vascular permeability (K_{trans}) and an increase in microvessel volume correlated with OS [51]. However, all of the above mentioned studies focused on changes in perfusion measurements measured before versus after anti-angiogenic therapy was initiated.

A challenge in assessing response to BV in glioma is that it will usually reduce BBB leakage, resulting in less contrast enhancement and edema. This phenomenon is known as pseudoresponse [52] and was observed only sporadically in our subjects. This causes important challenges in confidently identifying those subjects that progressed at 6 months. While antiangiogenics reduce edema, diffusion imaging can still identify tumor progression when enhancement ceases: viable tumor usually restricts diffusion while treated tumor or gliosis tends to have increased diffusion; therefore, an enlarging region of restricted diffusion usually means growth of tumor. The decision tree we propose shows that diffusion imaging is the most important factor in separating subjects (because they are at the top of the tree) but perfusion can help to separate those with less distinctive diffusion measurements.

It is interesting that diffusion was more important for predicting response to an anti-angiogenic agent than perfusion imaging. One might expect that tumors with high perfusion would have the most response potential. In fact, where perfusion was used in the decision tree, low perfusion tumors were more likely to respond, perhaps because the effect of the drug was to largely shut down perfusion to those tumors, while those with much perfusion still had enough blood flow that they were not impacted by BV.

Important limitations of this study include that the calculation of rCBV values is dependent on the software used [53]. While other software can likely also predict non-responsiveness to BV, each package will likely have different values. The software we used has been found to give results very similar to some other packages. The calculation of ADC values is well-known, but differences in filtering of ADC maps will impact histogram values, and thus must also be carefully evaluated when others attempt to replicate our work–we note here that we did not perform any filtering of the images.

Another limitation of this study is due to its retrospective character with only 54 subjects, yet with united BV regimen and steroid dose. The consistency of multiple classifiers helps to improve confidence, but does not guarantee that overfitting did not occur. The thresholds selected for the 3 categories (responder/possible/not responder) cannot be expected to be 100% accurate for the general population, and a

prospective analysis of this method should be considered.

We also evaluated the various image metrics used by the 6 classifiers that contributed to predictions. There were substantial differences in the image measurements used between OS and PFS6 prediction for a given machine learning method - e.g., the GB classifier in Fig. 2. One might expect that OS and PFS6 prediction should be related, and the lack of overlap suggests that the image measurements may be noisy, but unrelated biological factors might also account for this difference.

5. Conclusions

Anti-angiogenic agents appear to be useful only in specific population of patients with recurrent glioblastoma. MRI parameters of ADC and rCBV with the use of machine learning techniques can identify not negligible number of those patients who are highly unlikely to respond to BV therapy. This can be very helpful in selecting patients that either should or should not be treated with BV. Yet, prospective validation of the of the proposed classification approach to eliminate non-responders is warranted.

Acknowledgements

We wish to express our appreciation to the European Regional Development Fund (CZ.1.05/1.1.00/02.0123) for their support.

References

[1] R. Stupp, W.P. Mason, M.J. van den Bent, et al., Radiotherapy plus concomitant and adjuvant temozolomide for glioblastoma, N. Engl. J. Med. 352 (2005) 987–996.
[2] M. Weller, R. Stupp, M. Hegi, et al., Individualized targeted therapy for glioblastoma: fact or fiction? Cancer J. (Sudbury, Mass) 18 (2012) 40–44.
[3] R. Stupp, S. Taillibert, A.A. Kanner, et al., Maintenance therapy with tumor-treating fields plus Temozolomide vs Temozolomide alone for Glioblastoma: a randomized clinical trial, Jama 314 (2015) 2535–2543.
[4] O. Gallego, Nonsurgical treatment of recurrent glioblastoma, Current Oncol (Toronto, Ont) 22 (2015) e273–e281.
[5] M.R. Gilbert, J.J. Dignam, T.S. Armstrong, et al., A randomized trial of bevacizumab for newly diagnosed glioblastoma, N. Engl. J. Med. 370 (2014) 699–708.
[6] O.L. Chinot, W. Wick, W. Mason, et al., Bevacizumab plus radiotherapy–Temozolomide for newly diagnosed Glioblastoma, N. Engl. J. Med. 370 (2014) 709–722.
[7] N. Ferrara, K.J. Hillan, H.P. Gerber, et al., Discovery and development of bevacizumab, an anti-VEGF antibody for treating cancer, Nat. Rev. Drug Discov. 3 (2004) 391–400.
[8] H.S. Friedman, M.D. Prados, P.Y. Wen, et al., Bevacizumab alone and in combination with irinotecan in recurrent glioblastoma, J. Clin. Oncol. 27 (2009) 4733–4740.
[9] B.M. Ellingson, H.J. Kim, D.C. Woodworth, et al., Recurrent glioblastoma treated with bevacizumab: contrast-enhanced T1-weighted subtraction maps improve tumor delineation and aid prediction of survival in a multicenter clinical trial, Radiology 271 (2014) 200–210.
[10] W. Wick, A.A. Brandes, T. Gorlia, et al., EORTC 26101 phase III trial exploring the combination of bevacizumab and lomustine in patients with first progression of a glioblastoma, J. Clin. Oncol. 34 (2016) 2001.
[11] K. Chang, B. Zhang, X. Guo, et al., Multimodal imaging patterns predict survival in recurrent glioblastoma patients treated with bevacizumab, Neuro-oncology 18 (2016) 1680–1687.
[12] B.M. Ellingson, S. Sahebjam, H.J. Kim, et al., Pretreatment ADC histogram analysis is a predictive imaging biomarker for bevacizumab treatment but not chemotherapy in recurrent glioblastoma, AJNR Am. J. Neuroradiol. 35 (2014) 673–679.
[13] W.B. Pope, H.J. Kim, J. Huo, et al., Recurrent glioblastoma multiforme: ADC histogram analysis predicts response to bevacizumab treatment, Radiology 252 (2009) 182–189.
[14] P.Y. Wen, D.R. Macdonald, D.A. Reardon, et al., Updated response assessment criteria for high-grade gliomas: response assessment in neuro-oncology working group, J. Clin. Oncol. 28 (2010) 1963–1972.
[15] B.M. Ellingson, P.Y. Wen, T.F. Cloughesy, Modified criteria for radiographic response assessment in Glioblastoma clinical trials, Neurotherapeutics. 14 (2017) 307–320.
[16] P.D. Korfiatis, T.L. Kline, D.J. Blezek, et al., MIRMAID: a content management system for medical image analysis research, Radiographics. 35 (2015) 1461–1468.
[17] N.J. Tustison, B.B. Avants, P.A. Cook, et al., N4ITK: improved N3 bias correction, IEEE Trans. Med. Imaging 29 (2010) 1310–1320.
[18] P.A. Yushkevich, J. Piven, H.C. Hazlett, et al., User-guided 3D active contour segmentation of anatomical structures: significantly improved efficiency and reliability, NeuroImage 31 (2006) 1116–1128.
[19] B.B. Avants, N.J. Tustison, G. Song, et al., A reproducible evaluation of ANTs similarity metric performance in brain image registration, NeuroImage 54 (2011) 2033–2044.
[20] P. Korfiatis, T.L. Kline, Z.S. Kelm, et al., Dynamic susceptibility contrast-MRI quantification software tool: development and evaluation, Tomography. 2 (2016) 448–456.
[21] J.H. Friedman, Greedy function approximation: a gradient boosting machine, Ann. Stat. 29 (2001) 1189–1232.
[22] C. Cortes, V. Vapnik, Support-vector networks, Mach. Learn. 20 (1995) 273–297.
[23] W.-Y. Loh, Classification and Regression Trees, (2011).
[24] N.S. Altman, An introduction to kernel and nearest-neighbor nonparametric regression, Am. Stat. 46 (1992) 175–185.
[25] K. Crammer, O. Dekel, J. Keshet, et al., Online Passive-Aggressive Algorithms, (2006).
[26] S. Sperandei, Understanding logistic regression analysis, Biochemia Medica 24 (2014) 12–18.
[27] R. Kohavi, A study of cross-validation and bootstrap for accuracy estimation and model selection, Proceedings of the 14th International Joint Conference on Artificial Intelligence, Vol 2 Morgan Kaufmann Publishers Inc., Montreal, Quebec, Canada, 1995, pp. 1137–1143.
[28] S.K. Mukherji, Bevacizumab (Avastin), AJNR Am. J. Neuroradiol. 31 (2010) 235–236.
[29] A.D. Norden, G.S. Young, K. Setayesh, et al., Bevacizumab for recurrent malignant gliomas: efficacy, toxicity, and patterns of recurrence, Neurology 70 (2008) 779–787.
[30] H. Wheeler, J. Black, S. Webb, et al., Dehiscence of corticosteroid-induced abdominal striae in a 14-year-old boy treated with bevacizumab for recurrent glioblastoma, J. Child Neurol. 27 (2012) 927–929.
[31] P. Grossmann, V. Narayan, K. Chang, et al., Quantitative imaging biomarkers for risk stratification of patients with recurrent glioblastoma treated with bevacizumab, Neuro-Oncol 19 (2017) 1688–1697.
[32] P. Goyal, M. Tenenbaum, S. Gupta, et al., Survival prediction based on qualitative MRI diffusion signature in patients with recurrent high grade glioma treated with bevacizumab, Quant Imaging Med Surg. 8 (2018) 268–279.
[33] N. Galla, G. Chiang, S. Chakraborty, et al., Apparent diffusion coefficient changes predict survival after intra-arterial bevacizumab treatment in recurrent glioblastoma, Neuroradiology 59 (2017) 499–505.
[34] K.M. Field, P.M. Phal, G. Fitt, et al., The role of early magnetic resonance imaging in predicting survival on bevacizumab for recurrent glioblastoma: results from a prospective clinical trial (CABARET), Cancer 123 (2017) 3576–3582.
[35] Y. Mardor, Y. Roth, A. Ochershvilli, et al., Pretreatment prediction of brain tumors' response to radiation therapy using high b-value diffusion-weighted MRI, Neoplasia (New York, NY) 6 (2004) 136–142.
[36] R.N. Sawlani, J. Raizer, S.W. Horowitz, et al., Glioblastoma: a method for predicting response to antiangiogenic chemotherapy by using MR perfusion imaging–pilot study, Radiology 255 (2010) 622–628.
[37] R.J. Harris, T.F. Cloughesy, A.J. Hardy, et al., MRI perfusion measurements calculated using advanced deconvolution techniques predict survival in recurrent glioblastoma treated with bevacizumab, J. Neuro-Oncol. 122 (2015) 497–505.
[38] W.B. Pope, Predictive imaging marker of bevacizumab efficacy: perfusion MRI, Neuro-Oncol 17 (2015) 1046–1047.
[39] H.R. Cho, B. Hong, H. Kim, et al., Assessment of bevacizumab resistance increased by expression of BCAT1 in IDH1 wild-type glioblastoma: application of DSC perfusion MR imaging, Oncotarget 7 (2016) 69606–69615.
[40] P. Kickingereder, A. Radbruch, S. Burth, et al., MR perfusion-derived hemodynamic parametric response mapping of Bevacizumab efficacy in recurrent Glioblastoma, Radiology 279 (2016) 542–552.
[41] I.E. Bennett, K.M. Field, C.M. Hovens, et al., Early perfusion MRI predicts survival outcome in patients with recurrent glioblastoma treated with bevacizumab and carboplatin, J. Neuro-Oncol. 131 (2017) 321–329.
[42] A. Hilario, J.M. Sepulveda, A. Hernandez-Lain, et al., Leakage decrease detected by dynamic susceptibility-weighted contrast-enhanced perfusion MRI predicts survival in recurrent glioblastoma treated with bevacizumab, Clin. Transl. Oncol. 19 (2017) 51–57.
[43] T.T. Liu, A.S. Achrol, L.A. Mitchell, et al., Magnetic resonance perfusion image features uncover an angiogenic subgroup of glioblastoma patients with poor survival and better response to antiangiogenic treatment, Neuro-Oncol 19 (2017) 997–1007.
[44] G. Bergers, D. Hanahan, Modes of resistance to anti-angiogenic therapy, Nat. Rev. Cancer 8 (2008) 592–603.
[45] P. Carmeliet, R.K. Jain, Molecular mechanisms and clinical applications of angiogenesis, Nature 473 (2011) 298–307.
[46] D.R. Macdonald, T.L. Cascino, S.C. Schold Jr.et al., Response criteria for phase II studies of supratentorial malignant glioma, J. Clin. Oncol. 8 (1990) 1277–1280.
[47] A.G. Sorensen, T.T. Batchelor, P.Y. Wen, et al., Response criteria for glioma, Nat. Clin. Pract. Oncol. 5 (2008) 634–644.
[48] M.J. van den Bent, M.A. Vogelbaum, P.Y. Wen, et al., End point assessment in gliomas: novel treatments limit usefulness of classical Macdonald's criteria, J. Clin. Oncol. 27 (2009) 2905–2908.
[49] A.G. Sorensen, K.E. Emblem, P. Polaskova, et al., Increased survival of glioblastoma patients who respond to antiangiogenic therapy with elevated blood perfusion, Cancer Res. 72 (2012) 402–407.
[50] T.T. Batchelor, E.R. Gerstner, K.E. Emblem, et al., Improved tumor oxygenation and survival in glioblastoma patients who show increased blood perfusion after cediranib and chemoradiation, Proc. Natl. Acad. Sci. U. S. A. 110 (2013) 19059–19064.
[51] A.G. Sorensen, T.T. Batchelor, W.-T. Zhang, et al., A "vascular normalization index" as potential mechanistic biomarker to predict survival after a single dose of Cediranib in recurrent Glioblastoma patients, Cancer Res. 69 (2009) 5296–5300.
[52] L.C. Hygino da Cruz Jr., I. Rodriguez, R.C. Domingues, et al., Pseudoprogression and pseudoresponse: imaging challenges in the assessment of posttreatment glioma, AJNR Am. J. Neuroradiol. 32 (2011) 1978–1985.
[53] Z.S. Kelm, P.D. Korfiatis, R.K. Lingineni, et al., Variability and accuracy of different software packages for dynamic susceptibility contrast magnetic resonance imaging for distinguishing glioblastoma progression from pseudoprogression, J. Med. Imaging (Bellingham, Wash) 2 (2015) 026001.